

**A COMPARATIVE STUDY OF DIFFERENT ARTIFICIAL INTELLIGENCE MODELS AND RESPONSE SURFACE METHODOLOGY FOR HEPTACHLOR REMOVAL USING FE/CU NANOPARTICLES**

Wan Sieng Yeo<sup>a,b\*</sup>

<sup>a</sup>Chemical and Energy Engineering Department, Faculty of Engineering and Science, Curtin University Malaysia, CDT 250, 98009 Miri, Sarawak, Malaysia

<sup>b</sup>Curtin Malaysia Research Institute, Curtin University, Malaysia

**Article history**

Received

20 June 2023

Received in revised form

15 August 2023

Accepted

20 August 2023

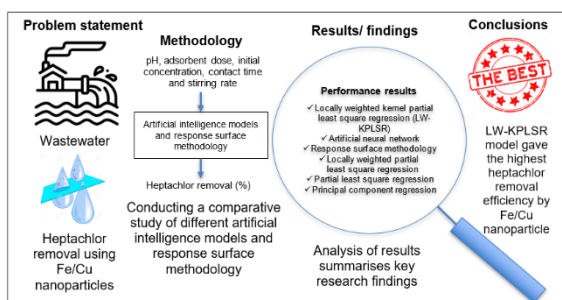
Published online

30 November 2023

\*Corresponding author

christineyeo@curtin.edu.my

**Graphical abstract**



**Abstract**

Water is a basic and essential resource in the human body. Every structure in the body including cells, tissues and organs needs water to work properly. Hence, without food, humans can last up to several weeks, but just a few days without water. Meanwhile, before water is consumed by a human's body, harmful impurities such as heptachlor which is a highly toxic organochlorine compound in the water must be removed. To remove heptachlor from the wastewater, the adsorption using the bimetallic iron/copper (Fe/Cu) nanoparticles can be a solution. However, the effectiveness of the elimination of heptachlor using the Fe/Cu nanoparticles could be affected by environmental factors including pH, adsorbent dosage, contact time, initial adsorbate concentration, and stirring rate. Response surface methodology (RSM) is widely used to correlate these factors with the heptachlor removal efficiency to achieve performance optimisation. However, the artificial intelligence models may perform better than RSM to optimise the heptachlor removal process. Therefore, this study aims to compare the performance of different artificial intelligence models with RSM for heptachlor removal using Fe/Cu nanoparticles. These different artificial intelligence models include principal component regression (PCR), artificial neural network (ANN), locally weighted kernel partial least square regression (LW-KPLSR), partial least square regression (PLSR), and least-square support vector regression (LSSVR). Based on the obtained results, the LW-KPLSR model performed better than other artificial intelligence models and RSM. Its root means square error, and mean absolute error are around 159% to 3,297% lower than other models and RSM. Moreover, its coefficient of determination which is so-called  $R^2$  is the highest among others. These results denote that LW-KPLSR is more convincing as compared to RSM to predict optimum performance of heptachlor removal.

**Keywords:** Wastewater treatment, heptachlor removal, artificial intelligence models, response surface methodology, Fe/Cu nanoparticles.

© 2023 Penerbit UTM Press. All rights reserved

**1.0 INTRODUCTION**

Water is vital to life and a basic human need. Therefore, good water sources management practices are required to ensure the waters are available, usable, and treated properly to provide a sufficient water supply including drinking water for the people. It was recorded that 844 million people lack of a basic drinking water supply in the year 2015 [1]. In future, the water demand is projected to increase from 20 to 30% above the current water level by the year 2050 due to population growth, socio-economic development, and drinking water accessibility which are still major concerns around the world [2]. Besides, there are around

1.5 to 12 million people who die yearly from waterborne and diarrheal diseases which are labelled among the dominant causes of death at a global level [3]. It is strictly necessary to remove pathogenic organisms, fatal matters, suspended solids, algae, organic matter, and harmful chemicals from wastewater to reduce the risks of waterborne and diarrheal diseases as well as making water safe for human consumption.

Heptachlor is one of the notable pollutants that exist in the wastewater which brings a negative impact on the ecological environment, humans, and animals which are human's food sources [4]. There is no doubt that heptachlor is a useful organochlorine pesticide employed for agricultural purposes,

seed treatment, wood preservatives against termites, and insect control [5, 6]. However, despite the benefits of using heptachlor such as its high efficiency and low cost [7], it could pollute the soil systems and aquatic ecosystem due to its toxicity [8]. Moreover, it could lead to cancer risk and it has distribution and bioaccumulation effects throughout the food chain [9]. To address this issue, bimetallic iron/copper (Fe/Cu) nanoparticles have been studied by Mahmoud et al. [10] to remove the heptachlor. Besides, Fe/Cu has been recently used by researchers such as Chan et al. [11], Mahmoud et al. [12], and Mahmoud and Mahmoud [13] to treat other pollutants such as ammonia and chemical oxygen demand. However, the effectiveness of the elimination of heptachlor using the Fe/Cu nanoparticles could be affected by environmental factors including pH, adsorbent dosage, initial adsorbate concentration, contact time, and stirring rate. Moreover, a review study conducted by Ngu et al. [14] discovered that response surface methodology (RSM) and artificial neural network (ANN) are the famous mathematical models used in researches related to nanoparticle and wastewater treatment. However, the prediction with these existing mathematical models may not be optimized results for the wastewater treatment.

On the other hand, response surface methodology (RSM) is a famous method that is used to correlate these environmental factors with the heptachlor removal efficiency to attain optimum performance. Nevertheless, the artificial intelligence (AI) models could be outperformed than RSM to maximise the heptachlor removal process. Hence, this research aims to compare the capability of the existing different AI models with RSM for heptachlor removal using Fe/Cu nanoparticles with the intention to introduce more machinery learning models for heptachlor removal using Fe/Cu nanoparticles. Rather than RSM and ANN which were widely used, other AI models like LW-KPLSR, PLSR, and PCR could be better choices. To select the best AI model, in this study, a comparison of the performance of ANN, RSM, LW-KPLSR, PLSR, and PCR was carried out. Then, an optimisation for heptachlor removal using Fe/Cu nanoparticles via adsorption process can be predicted using an AI model. In this study, the predictive performance of ANN, locally weighted kernel partial least square regression (LW-KPLSR), partial least square regression (PLSR), least-square support vector regression (LSSVR), and principal component regression were assessed and compared using a case study of the Heptachlor removal using Fe/Cu nanoparticles.

## 2.0 METHODOLOGY

In this study, a comparative study of different AI models and RSM for heptachlor removal using Fe/Cu nanoparticles was done. This section presents the research methodology of this study which includes the case study of heptachlor removal using Fe/Cu nanoparticles, LW-KPLSR, ANN, LSSVR, PCR, PLSR, RSM, models' quality prediction evaluation, and software and computer configurations.

### 2.1 Case Study Of The Heptachlor Removal Using Fe/Cu Nanoparticles

The case study used in this study was adopted from Mahmoud et al. [10]. In their study, the Fe/Cu nanoparticles were utilised

to remove heptachlor from an aqueous solution. They found that the optimal heptachlor elimination performance is 99.3% at the pH of 7 with 0.33 g/L of Fe/Cu, 2 µg/L of initial heptachlor amount, 30 minutes of contact time, and 250 rotations per minute (rpm) of stirring rate. This result has proven that Fe/Cu is an effective adsorbent to remove heptachlor from a solution due to its high efficiency for the adsorption of heptachlor. Besides, there are numerous environmental factors including adsorbent dosage, pH, initial adsorbate concentration, stirring rate, and contact time that influence the Heptachlor absorption using Fe/Cu and then influence the heptachlor elimination effectiveness. Therefore, the correlation between these environmental factors and the heptachlor removal efficiency is able to be investigated using AI models or RSM. These models or methods can be used to predict the optimum adsorption performance of Fe/Cu nanoparticles in removing heptachlor compounds under different environmental or experimental conditions.

### 2.2 Locally Weighted Kernel Partial Least Square Regression (LWKPLSR) Model

In the LW-KPLS model, by applying an appropriate Kernel function, the data of the case study are mapped into an infinite-dimensional space. In this study, the mapping of the case study's data into an infinite-dimensional space was done using the log Kernel function displayed in Equation (1) [15, 16].

$$k(x, x_i) = -\log(\|x - x_i\|^b + 1) \quad (1)$$

where  $b$  is the kernel parameter that is required to be tuned to get an optimum result from the LW-KPLSR. In this study, the fine-tuned  $b$  for the LW-KPLSR is 0.001.

Besides, in this model, the independent or input and dependent or output matrices are symbolised by  $x_n \in R^{n \times M}$  and  $y_n \in R^{n \times L}$ , respectively in which  $n$ ,  $M$ ,  $L$ , and  $T$  are the number of samples, the amount of independent or input variables, the amount of dependent or output variables, and a transpose of a matrix, respectively. On the other hand,  $\hat{y}_q$  is the predicted dependent or output for a query,  $x_q$ . To determine a dependent or output variable, the log Kernel matrices for the independent or input variable,  $V$ , and query,  $V_q$  are initiated to map these variables into an infinite-dimensional feature space by using the log Kernel function. Later, Equations (2) and (3) are used to get the mean centering on the  $V$  and  $V_q$  [17].

$$\tilde{V} = \left( I - \frac{1}{n} \mathbf{1}_n \mathbf{1}_n^T \right) V \left( I - \frac{1}{n} \mathbf{1}_n \mathbf{1}_n^T \right) \quad (2)$$

$$\tilde{V}_q = \left( V_q - \frac{1}{n_t} \mathbf{1}_{n_t} \mathbf{1}_{n_t}^T V \right) \left( I - \frac{1}{n} \mathbf{1}_n \mathbf{1}_n^T \right) \quad (3)$$

where  $\mathbf{1}_n$  and  $\mathbf{1}_{n_t}$  are the length vector with  $n$  and the length vector with  $n_t$ , respectively. Meanwhile, Equation (4) is used to perform the dual KPLS discrimination to obtain the dual representation of the scaling in the projection direction,  $B$  [18].

$$B = Y Y' V \beta \text{ with normalization, } \beta = \frac{\beta}{\|\beta\|} \quad (4)$$

Later, the calculations of the re-scaled query and independent or input variable,  $V_q$  and  $V$  variables employing  $B$

are done, and Equations (5) and (6) are employed to reconstruct them.

$$x_q = V_q B \quad (5)$$

$$X = VB \quad (6)$$

Next, the latent variables number,  $s$  is adopted, and  $s$  is fixed at 1. Afterward, the similarity matrix,  $\Omega$  is computed via Equations (7) to (9).

$$\Omega = \text{dig}\{\omega_1, \omega_2, \dots, \omega_N\} \quad (7)$$

$$\omega_n = \exp\left(-\frac{d_n}{\varphi\sigma_n}\right) \quad (8)$$

$$d_n = \sqrt{(x_n - x_q)^T (x_n - x_q)} \quad (9)$$

where  $\omega_n$ ,  $\varphi$  and  $\sigma_n$  are the index of similarity describing the distance between  $x_n$  and  $x_q$ , the localisation parameter, and the standard deviation of  $d_n = (n = 1, 2, \dots, N)$ , respectively. In this study, the  $\varphi$  value is set as 0.1 as this value was suggested by Yeo et al. [19]. More information on the LW-KPLSR model is available in Yeo et al. [19] and Ngu and Yeo [18].

### 2.3 Artificial Neural Network (ANN) Model

Kuang et al. [20] reported that ANN is superior in handling nonlinear data, an ability that was lacking in linear models such as PLSR and PCR. Generally, an ANN model consists of a series of layers that are input, hidden, and output layers. The type of ANN used in this study is feedforward backpropagation ANN algorithm. In this study, the hidden layer has 10 neurons, and hence a structure of 5-10-1 was utilised to perform the prediction of an output. With a total of 24 datasets, input and output data were divided into 60% for training the ANN, 20% for ANN model validation, and 20% for testing the created ANN. More information about the ANN used in this study can be obtained from Mahmoud et al. [10]. The details about ANN models can be found in Abiodun et al. [21], and Zhang [22].

### 2.4 Partial Least Square Regression (PLSR) Model

PLSR can predict the values of an output variable,  $Y$  based on the trend of another input variable,  $X$  where both of these input and output variables are considered and correlated [23]. Consider two sets of data in two matrices to form  $X$  and  $Y$ . Both matrices contain  $n$  rows which means  $n$  observations.  $X$  has  $k$  columns which are the  $X$ -variables denoted by  $x_k$  while  $Y$  has  $m$  columns which are the  $Y$ -variables denoted by  $y_m$ . Estimates of the latent variables are computed by the PLSR model as  $a$ , the new variables. The new variables are named  $X$ -scores and designated by  $T$  as depicted in Equation (10) [24]:

$$T = XW^* \quad (10)$$

The  $X$ -scores represent predictors of  $Y$  and are used to model  $X$ . They are linear combinations of the original variables  $x_k$  with the coefficients named weights denoted by  $W^*$ . The  $X$ -scores,  $T$  are multiplied with the loadings,  $P$  to make the  $X$ -residuals,  $E$  small as illustrated in Equation (11):

$$X = TP^T + E \quad (11)$$

When  $Y$  has more than one variable, the  $Y$ -scores,  $U$  are added by the weights,  $C$  to make the residuals,  $G$  small as demonstrated in Equation (12):

$$Y = UC^T + G \quad (12)$$

Since the  $X$ -scores are good predictors of  $Y$ , they can be multiplied by the weights of  $Y$  as shown in Equation (13):

$$Y = TC^T + F \quad (13)$$

The difference between the observed and predicted  $Y$  is expressed by the  $Y$ -residuals,  $F$ . The presence of Equation (10) allows Equation (13) to be rewritten as demonstrated in Equation (14):

$$Y = XW^*C^T + F = XB + F \quad (14)$$

From Equation (14), the PLSR model coefficient matrix,  $B_{\text{PLSR}}$  can be written as depicted in Equation (15):

$$B_{\text{PLSR}} = W^*C^T \quad (15)$$

### 2.5 Principal Component Regression (PCR) Model

In PCR, a principal component analysis (PCA) is only working on  $X$ -variables as a first step. The  $Y$ -variables are then regressed on the principal components (PCs) obtained from the performing PCA of  $X$ . The regression and dimension reduction are combined in the algorithm of PCR. However, dimension reduction is only done on the predictor set  $X$  but not be done on the output or dependent variables. The number of factors or PCs,  $A$  is a requirement for PCR. Firstly, a PCA is carried out on centred  $X$  as depicted in Equation (16) [25]:

$$X = USV^T \quad (16)$$

Then, multivariate least squares regression of  $Y$  is done on the major  $A$  PCs utilising either the unit-norm singular vectors  $U_{[A]}$  or the PCs  $T_{[A]}$  as illustrated in Equation (17):

$$T_{[A]} = XU_{[A]} = U_{[A]}S_{[A]} \quad (17)$$

Each  $Y$ -variable is then projected onto the space spanned by the first  $A$  PCs of  $X$  which can be represented as Equation (18):

$$\hat{Y} = U_{[A]}U_{[A]}^T Y = T_{[A]}(T_{[A]}^T T_{[A]})^{-1} T_{[A]}^T Y \quad (18)$$

For the final step, the PCR model coefficient matrix,  $B_{\text{PCR}}$  having the size of  $p \times m$  is obtained in a few ways as described in Equation (19):

$$B_{\text{PCR}} = (X^T X)^{-1} X^T \hat{Y} = V_{[A]}S_{[A]}^{-1} U_{[A]}^T Y = V_{[A]}(T_{[A]}^T T_{[A]})^{-1} T_{[A]}^T Y \quad (19)$$

The vector of intercepts is then adopted and represented in Equation (20):

$$b = (m_Y^T - m_X^T B_{\text{PCR}})^T \quad (20)$$

### 2.6 Least Square Support Vector Regression (LSSVR) Model

The algorithm for LSSVR is considered a model in the primal weight space as shown in Equation (21) [26]:

$$y(x) = w^T \varphi(x) + b \quad (21)$$

where  $x \in \mathbb{R}^n$ ,  $y \in \mathbb{R}$  and  $\varphi(\cdot) : \mathbb{R}^n \rightarrow \mathbb{R}^{n_h}$  is the mapping to the feature space which is of higher or potential infinite dimensions. The below optimisation problem in the primal

weight space depicted in Equation (22) [27] is then formulated based on the data from the case study  $\{x_k, y_k\}_{k=1}^N$ :

$$\min_{w_0, V, b, e} J_p(w_0, V, e) = \frac{1}{2} w_0^T w_0 + \frac{\lambda}{N^2} \text{trace}(V^T V) + \gamma \frac{1}{2} \text{trace}(E^T E) \tag{22}$$

where  $w_0 \in \mathbb{R}^{n_h}$  carries information of the commonality, elements of  $V = (v_1, v_2, \dots, v_k) \in \mathbb{R}^{n_h \times k}$  carries information of the specialty,  $b = (b_1, b_2, \dots, b_k) \in \mathbb{R}^k$ ,  $\lambda, \gamma \in \mathbb{R}_+$  are non-negative real regularised parameters in which the tuned  $\lambda$  and  $\gamma$  in this study are 13 and 0, respectively. Moreover,  $E = (e_1, e_2, \dots, e_k) \in \mathbb{R}^{l \times k}$  is a vector containing slack variables. If  $A$  is a  $k \times k$  matrix,  $\text{trace}(A) = \sum_{i=1}^k A_{i,i}$ . Equation (22) is subjected to the equality constraints shown in Equation (23):

$$Y = Z^T W + \text{repmat}(b^T, l, 1) + E \tag{23}$$

where  $Z = (\varphi(x_1), \varphi(x_2), \dots, \varphi(x_l)) \in \mathbb{R}^{n_h \times l}$ ,  $W = (w_0 + v_1, w_0 + v_2, \dots, w_0 + v_k) \in \mathbb{R}^{n_h \times k}$  and  $\text{repmat}(A, m, n)$  produces a huge block matrix containing an  $m \times n$  tiling copies of  $A$ .

It is to note that the primal problem described in Equation (22) cannot be solved if  $w_0$  becomes infinite-dimensional. Thus, the Lagrangian need to be constructed as depicted in Equation (24):

$$\mathcal{L}(w_0, V, b, e; \alpha) = J_p(w_0, V, e) - \text{trace}(A^T (Z^T W + \text{repmat}(b^T, l, 1) + E - Y)) \tag{24}$$

where  $A = (\alpha_1, \alpha_2, \dots, \alpha_k) \in \mathbb{R}^{l \times k}$  is a matrix of Lagrange multipliers. Based on the Karush-Kuhn-Tucker optimal conditions and eliminating variables  $W$  and  $E$ , the dual problem for multi-output is derived as illustrated in Equations (25) and (26):

$$\begin{bmatrix} 0_{kl \times k} & P^T \\ P & H \end{bmatrix} \begin{bmatrix} b \\ \alpha \end{bmatrix} = \begin{bmatrix} 0_k \\ y \end{bmatrix} \tag{25}$$

$$\text{such that } H = \Omega + \frac{I_{kl}}{\gamma} + \binom{k}{\lambda} Q \in \mathbb{R}^{kl \times kl} \tag{26}$$

where  $P = \text{blockdiag}(\overbrace{(1_1, 1_1, \dots, 1_1)}^k) \in \mathbb{R}^{kl \times k}$ ,  $\Omega = \text{repmat}(K, k, k) \in \mathbb{R}^{kl \times kl}$ ,  $Q = \text{blockdiag}(\overbrace{(K, K, \dots, K)}^k) \in \mathbb{R}^{kl \times kl}$ ,  $K = Z^T Z \in \mathbb{R}^{l \times l}$  is denoted by its elements  $K_{i,j} = \phi(x_i)^T \phi(x_j) = \kappa(x_i, x_j)$ ,  $\text{blockdiag}(A_1, A_2, \dots, A_n)$  creates a block diagonal matrix containing  $A_1, A_2, \dots, A_n$  as main diagonal blocks, with other blocks being zero matrices,  $\alpha = (\alpha_1^T, \alpha_2^T, \dots, \alpha_k^T)^T \in \mathbb{R}^{kl}$  and  $y = (y_1^T, y_2^T, \dots, y_k^T)^T \in \mathbb{R}^{kl}$ . Therefore, the linear system in Equation (25) consists of  $(l + 1) \times k$  equations but it is difficult to solve since it is not positive definite. It is then reformulated as described in Equation (27):

$$\begin{bmatrix} S & 0_{kl \times kl} \\ 0_{k \times k} & H \end{bmatrix} \begin{bmatrix} b \\ H^{-1} P b + \alpha \end{bmatrix} = \begin{bmatrix} P^T H^{-1} y \\ y \end{bmatrix} \tag{27}$$

where  $S = P^T H^{-1} P \in \mathbb{R}^{k \times k}$ . The solution to Equation (27) can be found by following these steps. Firstly, solve  $\eta, v$  from  $H_\eta = P$  and  $H_v = y$ . Then, compute  $S = P^T \eta$ . Finally, determine the

solution from  $b = S^{-1} \eta^T y$  and  $\alpha = v - \eta b$ . The solution of Equation (25) is defined as  $\alpha^* = (\alpha_1^{*T}, \alpha_2^{*T}, \dots, \alpha_k^{*T})^T$  and  $b^*$ . This results in the LSSVR model for multi-outputs as depicted in Equation (28):

$$\hat{f}(x) = \text{repmat}(\sum_{i=1}^k \sum_{j=1}^l \alpha_{i,j}^* \kappa(x, x_j), 1, k) + \frac{k}{\lambda} \sum_{j=1}^l \alpha_j^* \kappa(x, x_j) + b^{*T} \tag{28}$$

### 2.7 Response Surface Methodology (RSM)

RSM is a famous method that is utilised to model and analyse a process that has a response of interest and this response can be affected by other variables [28]. Hence, the RSM is used to find the maximal response of the process, which is the optimum heptachlor removal efficiency in this study. Similar to the AI models, RSM is used to obtain the correlation describing the correlation of the environmental factors and heptachlor removal efficiency. The RSM is a linear multivariate polynomial regression equation shown in Equation (29) [29].

$$Y = \beta_0 + \beta_1 x_1 + \beta_2 x_2 + \beta_3 x_3 + \beta_4 x_4 + \beta_5 x_5 \tag{29}$$

where  $\beta_0$  is a constant for the regression equation. Moreover,  $\beta_1, \beta_2, \beta_3, \beta_4$ , and  $\beta_5$  are the corrected operating parameter values. Additionally,  $x_1, x_2, x_3, x_4$ , and  $x_5$  denote the operating parameter values while  $y$  is the removal efficiency. More details about RSM used in this study can be found in Mahmoud et al. [10].

### 3.0 MODELS DEVELOPMENT AND MODELS' QUALITY PREDICTION EVALUATION

In this study, there are a total of 24 datasets from an experimental work consisting of the environmental factors including pH, adsorbent dosage, initial adsorbate concentration, contact time, stirring rate, and heptachlor removal efficiency adopted from Mahmoud et al. [10] to develop the AI models and RSM. All of these models were using adsorbent dosage, pH, initial adsorbate concentration, stirring rate, and contact time as the input variables while their output variable is the percentage of heptachlor removal utilising Fe/Cu nanoparticles. These input and output variables were employed to construct the AI models and RSM. To assess the predictive performance of these models, the input variables which are the environmental factors were executed using these developed models to obtain the predicted percentage of heptachlor removal. Then, the root mean squared error (RMSE), mean absolute error (MAE), and coefficient of determination ( $R^2$ ) for that were denoted as the results from the AI models and RSM were determined and compared. Figure 1 shows the methodological framework of LW-KPLSR, ANN, LSSVR, PLSR, PCR, and RSM algorithms using MATLAB.

RMSE acts as a scale-dependent error metric that is frequently employed to assess the accuracy of the performance of models [30]. The formula for RMSE is exhibited in Equation (30) [31, 32].

$$RMSE = \sqrt{\frac{\sum_i (Y_i - \hat{Y}_i)^2}{n}} \quad (30)$$

where  $Y_i$  and  $\hat{Y}_i$  represented the real and estimated dependent or output while  $n$  is the number of samples.

Additionally, MAE is the measure of the mean of errors in a set of predictions regardless of the direction. The equation of MAE can be seen in Equation (31) [33].

$$MAE = \sum \frac{|y_i - \hat{y}_i|}{N_T} \quad (31)$$

Moreover,  $R^2$  is displayed in Equation (32) [34] and it accesses how good or strong a regression model describes the fraction of variance in the dataset [35].

$$R^2 = 1 - \frac{\sum_i (y_i - \hat{y}_i)^2}{\sum_i (y_i - \bar{Y})^2} \quad (32)$$

whereby  $\bar{Y}$  represents the average value of the actual output.

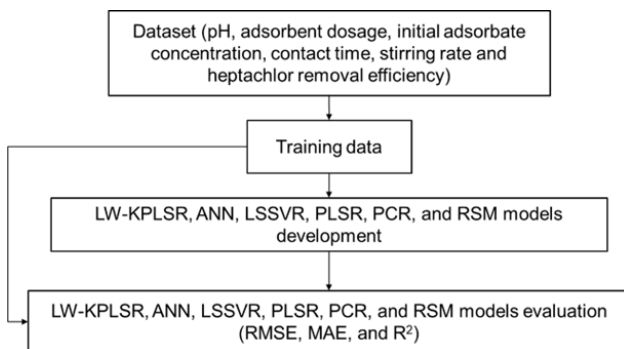


**Figure 1** The methodological framework of LW-KPLSR, ANN, LSSVR, PLSR, PCR, and RSM models using MATLAB.

In addition, prediction error ( $PE$ ) is applied to evaluate the difference between two results, and it is represented as Equation (33) as follows [36]:

$$PE = \left| \frac{V_1 - V_2}{V_1} \right| \times 100\% \quad (33)$$

where  $V_1$  and  $V_2$  are the targeted and observed values, respectively.

### 3.1 Software and Computer Configurations

The simulation works presented in this study were computed by an Acer Swift 5 Thin and Light Laptop Intel Core i7 11<sup>th</sup> gen. Its computer configuration specifications are Windows 10 Home 64 bits, 4.2 gigahertz Intel Core i7, 16.0 gigabyte RAM, and 512-gigabyte solid-state drive storage. Meanwhile, the software used in this laptop is MATLAB version R2021a.

## 4.0 RESULTS AND DISCUSSION

The results and discussion were carried out to compare and conclude the comparative prediction analysis of the results for heptachlor elimination effectiveness from the different AI models and RSM. The comparisons of these prediction results for

heptachlor removal efficiency from the five AI models including LW-KPLSR, ANN, LSSVR, PLSR, and PCR, as well as RSM, are shown in Table 1. From Table 1, in contrast to other models, LW-KPLSR obtained the best RMSE and MAE values which are 0.4675 and 0.3232, respectively. Its RMSE and MAE are about 159% to 3,297% lower than other models. Other than that, the  $R^2$  value for LW-KPLSR is 0.9991 ( $\sim 1.00$ ) and it is also the highest among other models. This is because LW-KPLSR consists of the log kernel function which can map the nonlinear data into an infinite dimensional space [15]. Moreover, this LW-KPLSR has a locally weighted algorithm that enables it to cope better with nonlinear data, collinear data, and outliers [36]. Apart from that, both ANN and LSSVR have better results than RSM, PLSR, and PCR since their  $R^2$  values are higher than 0.86. However, the predictive performance of these models, especially ANN could greatly degrade with the presence of outliers [37]. On the other hand, the RSM that utilises a linear polynomial regression equation is unable to handle the nonlinear data in this study even though it correlates all of the environmental factors of the adsorption of heptachlor in its equation. Besides, both PLSR and PCR performed badly in this study since they acquire less nonlinear information than other models [38].

**Table 1** Comparison of the prediction results for heptachlor removal efficiency from AI models and RSM.

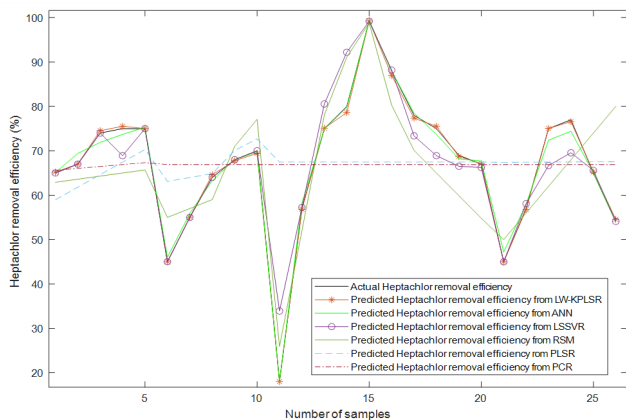
Models	LW-KPLSR	ANN	LSSVR	RSM	PLSR	PCR
RMSE	0.47	1.21	5.04	9.18	15.16	15.38
MAE	0.32	0.86	2.76	7.66	10.92	10.98
$R^2$	$\sim 1.00$	0.99	0.87	0.57	-31.84	-2,387.56

Figure 2 displays the prediction results of the heptachlor removal efficiency using five different AI models and RSM. Notice that the heptachlor removal efficiencies using Fe/Cu nanoparticles are fallen between approximately 18% to 99%. Furthermore, Figure 2 shows that the predicted heptachlor removal efficiencies from RSM, PLSR, and PCR are far from their actual values. Although the predicted heptachlor removal efficiencies from ANN and LSSVR are better than RSM, PLSR, and PCR since their values are closer to their actual values, their predictive performances are not as good as the predicted heptachlor removal efficiencies from LW-KPLSR. From Figure 2, it is very obvious that LW-KPLSR produces the almost identical predicted heptachlor removal efficiencies as their actual values. Figure 3 shows the correlation between the real and predicted values of the heptachlor removal efficiency using the LW-KPLSR model. From Figure 3, notice that both actual and predicted values of the heptachlor removal efficiency are very similar. It can conclude that LW-KPLSR outperformed other models in predicting the heptachlor removal efficiencies using Fe/Cu nanoparticles.

## 5.0 CONCLUSION

Adsorption using the bimetallic Fe/Cu nanoparticles has been recognised as an effective method to remove a pollutant, namely heptachlor from wastewater. Heptachlor is an organochlorine compound that was used as an insecticide and it is a highly to moderately toxic compound that harms the liver, nervous system, reproductive capacity, and the developing

offspring after short-term oral exposure. However, its effectiveness could be affected by environmental factors including adsorbent dosage, pH, initial adsorbate concentration, stirring rate, and contact time. And RSM is usually used to optimize the adsorption of Fe/Cu nanoparticles, however, it may not be a good method for optimisation of the removal of heptachlor. Hence, this study investigated the performance of the LW-KPLSR, ANN, LSSVR, PLSR, PCR, and RSM for heptachlor removal utilising Fe/Cu nanoparticles. A comparison was conducted between these models in terms of accuracy, which was validated via RMSE, MAE, and  $R^2$ . Based on the results obtained, it is shown that LW-KPLSR provided the best predictive results in comparison with other models. Its RMSE and MAE are 159% to 3,297% lower than other models. In addition, among all the models, the  $R^2$  value for LW-KPLSR is the highest, which is 0.9991 (~1.00). In conclusion, LW-KPLSR is the most suitable model for predicting the heptachlor removal efficiencies using Fe/Cu nanoparticles.



**Figure 2** Prediction results of the heptachlor removal efficiency using five different AI models and RSM.

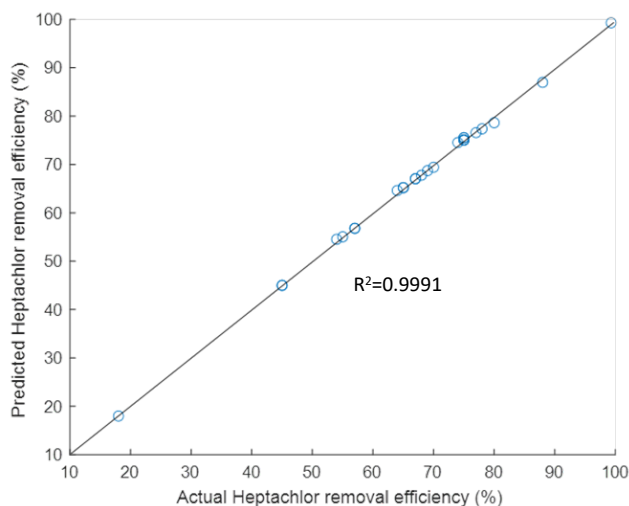


**Figure 3** Correlation between the real and estimated values of the heptachlor removal efficiency using the LW-KPLSR model.

### Acknowledgement

The author thanks Curtin Malaysia Research Institute Collaborative Research Scheme (CMRI-CRS) 2021, Curtin

University Malaysia, and SEGi University Malaysia since they provide financial support for this project. The author declares that there is no conflict of interest regarding the publication of this paper.

### References

- [1] Prüss-Ustün, A., et al., 2019. Burden of disease from inadequate water, sanitation and hygiene for selected adverse health outcomes: an updated analysis with a focus on low-and middle-income countries. *International Journal of Hygiene and Environmental Health* 222(5): 765-777. <https://doi.org/10.1016/j.ijheh.2019.05.004>
- [2] Xu, X., et al., 2020. Projecting China's future water footprint under the shared socio-economic pathways. *Journal of Environmental Management* 260: 110102. DOI: <https://doi.org/10.1016/j.jenvman.2020.110102>
- [3] Xagoraki, I. and E. O'Brien, 2020. Wastewater-based epidemiology for early detection of viral outbreaks. *Women In Water Quality*, 75-97. Springer. [https://doi.org/10.1007/978-3-030-17819-2\\_5](https://doi.org/10.1007/978-3-030-17819-2_5)
- [4] Topal, T. and C. Onac, 2020. Determination of heavy metals and pesticides in different types of fish samples collected from four different locations of aegean and marmara sea. *Journal of Food Quality* 2020: 1-12. <https://doi.org/10.1155/2020/8101532>
- [5] Authority, E. F. S., 2007. Opinion of the Scientific Panel on contaminants in the food chain [CONTAM] related heptachlor as an undesirable substance in animal feed. *European Food Safety Authority (EFSA) Journal* 5(6): 478. <https://doi.org/10.2903/j.efsa.2007.478>
- [6] Leong, K. H., et al., 2007. Contamination levels of selected organochlorine and organophosphate pesticides in the Selangor River, Malaysia between 2002 and 2003. *Chemosphere* 66(6): 1153-1159. <https://doi.org/10.1016/j.chemosphere.2006.06.009>
- [7] Cortada, C., et al., 2009. Determination of organochlorine pesticides in complex matrices by single-drop microextraction coupled to gas chromatography-mass spectrometry. *Analytica Chimica Acta* 638(1): 29-35. <https://doi.org/10.1016/j.aca.2009.01.062>
- [8] Bhuvanewari, R., et al., 2021. Chemisorption of Heptachlor and Mirex molecules on beta arsenene nanotubes—A first-principles analysis. *Applied Surface Science*. 537: 147835. <https://doi.org/10.1016/j.apsusc.2020.147835>
- [9] Zhang, G., et al., 2014. Distribution and bioaccumulation of organochlorine pesticides (OCPs) in food web of Nansi Lake, China. *Environmental Monitoring and Assessment* 186(4): 2039-2051. <https://doi.org/10.1007/s10661-013-3516-5>
- [10] Mahmoud, A. S., et al., 2020. Isotherm and kinetic studies for heptachlor removal from aqueous solution using Fe/Cu nanoparticles, artificial intelligence, and regression analysis. *Separation Science and Technology*, 55(4): 684-696. <https://doi.org/10.1080/01496395.2019.1574832>
- [11] Chan, M., et al., 2021. Oxidation of ammonia using immobilised FeCu for water treatment. *Separation and Purification Technology* 254: 117612. <https://doi.org/10.1016/j.seppur.2020.117612>
- [12] Mahmoud, A. S., et al., 2021. A prototype of textile wastewater treatment using coagulation and adsorption by Fe/Cu nanoparticles: Techno-economic and scaling-up studies. *Nanomaterials and Technologies for Environmental Applications* 11: 1-21. <https://doi.org/10.1177/18479804211041181>
- [13] Mahmoud, M. and A. S. Mahmoud, 2021. Wastewater treatment using nano bimetallic iron/copper, adsorption isotherm, kinetic studies, and artificial intelligence neural networks. *Emergent Materials* 4(5): 1455-1463. <https://doi.org/10.1007/s42247-021-00253-y>
- [14] Ngu, J. C. Y., et al., 2023. The application of machine learning in nanoparticle treated water: A review. *Curtin Global Campus Higher Degree by Research Colloquium (CGCHDC 2022)*, MATEC Web of Conference. <https://doi.org/10.1051/mateconf/202337701009>
- [15] Yeo, W. S., et al., 2019. Adaptive soft sensor development for non-Gaussian and nonlinear processes. *Industrial Engineering Chemistry Research*. 58(45): 20680-20691. <https://doi.org/10.1021/acs.iecr.9b03821>

- [16] Malang, J., et al., 2023. A comparison study between different kernel functions in the least square support vector regression model for penicillin fermentation process. *Curtin Global Campus Higher Degree by Research Colloquium (CGCHDR 2022)*, Miri, Sarawak, Malaysia, MATEC Web of Conferences <https://doi.org/10.1051/mateconf/202337701025>
- [17] Pervez, M., et al., 2023. Prediction of the Diameter of Biodegradable Electrospun Nanofiber Membranes: An Integrated Framework of Taguchi Design and Machine Learning. *Journal of Polymers the Environment*. 1-17. <https://doi.org/10.1007/s10924-023-02837-7>
- [18] Ngu, J. C. Y. and W. S. Yeo, 2023. A comparative study of different kernel functions applied to LW-KPLS model for nonlinear processes. *Biointerface Research in Applied Chemistry*. 13(2): 1-16. <https://doi.org/10.33263/BRIAC132.184>
- [19] Yeo, W. S., et al., 2017. Development of adaptive soft sensor using locally weighted kernel partial least square model. *Chemical Product and Process Modeling* 12(4): 1-13. <https://doi.org/10.1515/cppm-2017-0022>
- [20] Kuang, B., et al., 2015. Comparison between artificial neural network and partial least squares for on-line visible and near infrared spectroscopy measurement of soil organic carbon, pH and clay content. *Soil and Tillage Research* 146(Part B): 243-252. <https://doi.org/10.1016/j.still.2014.11.002>
- [21] Abiodun, O. I., et al., 2018. State-of-the-art in artificial neural network applications: A survey. *Heliyon* 4(11): e00938. <https://doi.org/10.1016/j.heliyon.2018.e00938>
- [22] Zhang, Z., 2018. Artificial neural network. Multivariate time series analysis in climate and environmental research, 1-35. Springer. [https://doi.org/10.1007/978-3-319-67340-0\\_1](https://doi.org/10.1007/978-3-319-67340-0_1)
- [23] Yeo, W. S., 2021. Prediction of Yellowness Index Using Partial Least Square Regression Model. *2021 International Conference on Green Energy, Computing and Sustainable Technology (GECOST)*, IEEE. <https://doi.org/10.1109/GECOST52368.2021.9538723>
- [24] Wold, S., et al., 2001. PLS-regression: a basic tool of chemometrics. *Chemometrics and Intelligent Laboratory Systems* 58(2): 109-130. [https://doi.org/10.1016/S0169-7439\(01\)00155-1](https://doi.org/10.1016/S0169-7439(01)00155-1)
- [25] Vandeginste, B. M., et al., 1998. Handbook of Chemometrics and Qualimetrics. *Data handling in science and technology* 20B. [https://doi.org/10.1016/S0922-3487\(98\)80045-2](https://doi.org/10.1016/S0922-3487(98)80045-2)
- [26] Suykens, J., et al., 2002. Least squares support vector machines. Singapore, World Scientific Publishing.
- [27] Xu, S., et al., 2013. Multi-output least-squares support vector regression machines. *Pattern Recognition Letters* 34(9):1078-1084. <https://doi.org/10.1016/j.patrec.2013.01.015>
- [28] Shahmansouri, A. A., et al., 2021. Mechanical properties of GGBFS-based geopolymer concrete incorporating natural zeolite and silica fume with an optimum design using response surface method. *Journal of Building Engineering* 36: 102138. <https://doi.org/10.1016/j.job.2020.102138>
- [29] Montgomery, D. C., et al., 2021. Introduction to linear regression analysis, John Wiley & Sons.
- [30] Morley, S. K., et al., 2018. Measures of model performance based on the log accuracy ratio. *Space Weather* 16(1): 69-88. <https://doi.org/10.1002/2017SW001669>
- [31] Thien, T. F. and W. S. Yeo, 2021. A comparative study between PCR, PLSR, and LW-PLS on the predictive performance at different data splitting ratios. *Chemical Engineering Communications*. 1-18. <https://doi.org/10.1080/00986445.2021.1957853>
- [32] Pervez, M. N., et al., 2023. Sustainable fashion: Design of the experiment assisted machine learning for the environmental-friendly resin finishing of cotton fabric. *Heliyon* 9(1): e12883. <https://doi.org/10.1016/j.heliyon.2023.e12883>
- [33] Willmott, C. J. and K. Matsuura, 2005. Advantages of the mean absolute error (MAE) over the root mean square error (RMSE) in assessing average model performance. *Climate research* 30(1): 79-82. <https://doi.org/10.3354/cr030079>
- [34] Yeo, W. S., et al., 2020. Missing data treatment for locally weighted partial least square-based modelling: A comparative study. *Asia-Pacific Journal of Chemical Engineering* 15(2): 1-13. <https://doi.org/10.1002/apj.2422>
- [35] Pizarro Inostroza, M. G., et al., 2020. Software-Automatized Individual Lactation Model Fitting, Peak and Persistence and Bayesian Criteria Comparison for Milk Yield Genetic Studies in Murciano-Granadina Goats. *Mathematics* 8(9): 1505. <https://doi.org/10.3390/math8091505>
- [36] Yeo, W. S. and W. J. Lau, 2021. Predicting the whiteness index of cotton fabric with a least squares model. *Cellulose* 28: 8841–8854 <https://doi.org/10.1007/s10570-021-04096-y>
- [37] Chakravarty, S., et al., 2020. Fuzzy regression functions with a noise cluster and the impact of outliers on mainstream machine learning methods in the regression setting. *Applied Soft Computing* 96: 106535. <https://doi.org/10.1016/j.asoc.2020.106535>
- [38] Liu, Y., et al., 2012. Just-in-time kernel learning with adaptive parameter selection for soft sensor modeling of batch processes. *Industrial & Engineering Chemistry Research* 51(11): 4313-4327. <https://doi.org/10.1021/ie201650u>